Biochimica et Biophysica Acta, 945 (1988) 145–160
Elsevier

BBA 74193

Thermodynamic-geometric correlations for the morphology of self-assembled structures of glycosphingolipids and their mixtures with dipalmitoylphosphatidylcholine

Bruno Maggio [b], John Albert [a] and Robert K. Yu [a]

[a] *Department of Neurology, Yale University School of Medicine, New Haven, CT (U.S.A.)* and [b] *Departamento de Quimica Biologica-CIQUIBIC, Facultad de Ciencias Quimicas-CONICET, Cordoba (Argentina)*

(Received 25 April 1988)

Key words: Glycosphingolipid; Ganglioside; Dipalmitoylphosphatidylcholine; Membrane morphology; Thermodynamics; Geometrics

The morphology of aqueous dispersions of five neutral glycosphingolipids (GalCer, GlcCer, LacCer, asialo-G_{M2}, asialo-G_{M1}), sulfatide, and five gangliosides (G_{M3}, G_{M2}, G_{M1}, G_{D1a} and G_{T1b}) and their mixtures with dipalmitoylphosphatidylcholine was studied by negative staining electron microscopy. The morphological features are interpreted on the basis of thermodynamic and geometric constraints previously studied in these systems (Maggio, B (1985) Biochim. Biophys. Acta 815, 245–258). The correlation between the theoretical predictions and the experimental findings are in reasonable agreement. Small changes in the molecular parameters of the individual glycosphingolipids or in their proportion in mixtures with dipalmitoylphosphatidylcholine bring about remarkable variations on the type of structure formed, its radius of curvature and thermodynamic stability.

Introduction

The pioneering work of Tanford [1,2] on the thermodynamics of self-association of amphiphiles in aqueous solutions was further developed by considering more explicitly the molecular geometry by Israelachvili and collaborators [3,4]. These studies have demonstrated that the shape of a multimolecular lipid structure is due to a balance of simultaneous constraints imposed on the lipid-water system by the molecular geometry, interacting free energies and entropy.

A theoretical discussion of the possible structure of model membrane systems containing neutral and anionic glycosphingolipids employing

Abbreviations: Cer, ceramide (*N*-acylsphingoid); GalCer, Galβ1–1Cer; GlcCer, Glcβ1–1Cer; LacCer, Galβ1–4Glcβ1–1Cer; Gg_3Cer (asialo-G_{M2}), GalNAcβ1–4Galβ1–4Glcβ1–1Cer; Gg_4Cer (asialo-G_{M1}), Galβ1–3GalNAcβ1–4Galβ1–4Glcβ1–1Cer; Gb_4Cer (globoside), GalNAcβ1–4Galα1–4Galβ1–4Glcβ1–1Cer; NeuAc, *N*-acetylneuraminate; sulfatide, Gal(3-sulfate)β1–1Cer; G_{M3}, NeuAcα2–3Galβ1–4Glcβ1–1Cer; G_{M2}, GalNAcβ1–4Gal(3–2αNeuAc)β1–4Glcβ1–1Cer; G_{M1}, Galβ1–3GalNAcβ1–4Gal(3–2αNeuAc)β1–4Glcβ1–1Cer; G_{D1a}, NeuAcα2–3Galβ1–3GalNAcβ1–4Gal(3–2αNeuAc)β1–4Glcβ1–1Cer; G_{T1b}, NeuAcα2–3Galβ1–3GalNAcβ1–4Gal(3–2αNeuAc8–2αNeuAc)β1–4Glcβ1–1Cer; DPPC, dipalmitoylphosphatidylcholine.

Correspondence: B. Maggio, Departamento de Quimica Biologica-CIQUIBIC, Facultad de Ciencias Quimicas-CONICET, Casilla de Correo 61, 5016 Cordoba, Argentina.

these criteria and experimental studies on several factors that can influence the transverse or lateral topography, shape and stability of these aggregates have been previously published [5–11]. In the present work we have studied directly by negative staining electron microscopy the morphology adopted by several glycosphingolipids and their mixtures with DPPC in different proportions; these features are interpreted on the basis of the thermodynamic and geometric properties of glycosphingolipid molecules. The results indicate that, at least in its overall features, the Tanford-Israelachvili approach for the self-association of lipid amphiphiles is in agreement with the morphological features found for systems containing glycosphingolipids in aqueous solution. This provides a useful framework within which alterations in membrane morphology, stability and function induced by glycosphingolipids can be more clearly understood.

Materials and Methods

Bovine brain GalCer, sulfatide and GlcCer from Gaucher spleen were purchased from Analab, North Haven, CT. DPPC was from Avanti Inc. Birmingham, AL. Gangliosides G_{M2}, G_{M1}, G_{D1a} and G_{T1b} were purified from bovine brain by DEAE-Sephadex and Iatrobeads column chromatographies as described elsewhere [12,13]. LacCer and G_{M3} were purified from bovine adrenal medulla [14].

Gangliotetraosylceramide (Gg_4Cer or asialo-G_{M1}) from bovine brain and gangliotriosylceramide (Gg_3Cer or asialo-G_{M2}) from human brain were obtained from a ganglioside mixture by mild formic acid desialylation followed by purification on an Iatrobeads column [15]. The purity of the glycosphingolipids was at least 95% as judged by HPTLC [16]. All solvents were freshly distilled before use and chemicals were of analytical reagent grade.

Lipid dispersions were prepared by pipetting the proper amount of lipid from chloroform-methanol (2:1, v/v) solutions into round-bottom tubes. The solvent was evaporated under a stream of N_2 and the lipid was heated to 55°C for 1 h and dried under vacuo for at least 4 h. Aqueous dispersions (1–7 mg/ml) were prepared as previously described [17] by hydrating the lipids for 5 min at 95°C, vortexed gently (at the lower speed setting) twice for 1 min each with an interval of 2 min during which the samples were kept at 95°C, vortexed again for 1 min and left at 22°C for 1 h before processing for negative staining. This treatment led to a reproducible and stable phase behavior as judged by high-sensitivity differential scanning calorimetry at low scan rates [17]. The procedure was strictly standardized and performed equally for all the dispersions; sonication was avoided in order to study the spontaneous shape adopted. HPTLC analysis performed after this treatment or after the negative staining procedure gave no evidence of degradation or contamination and the samples showed a similar morphology after being kept for several days at 4°C.

The negative staining solution was selected by studying the behavior of the lipid dispersions with sodium phosphotungstate, sodium silicotungstate or sodium phosphomolybdate at a concentration of 2% (w/v). The osmolarity was kept at 300 mosM with NaCl. Three different methods for negative staining were examined: (a) the lipids were dispersed directly into the solution containing the negative stain and this preparation was transferred to a pure carbon film produced by flash evaporation of carbonized yarn onto freshly cleaved and glow discharged mica sheets and then to uncoated 300 mesh copper grids for observation, after draining the excess solutions with filter paper in the usual manner; (b) a drop of the lipid dispersion prepared in the NaCl solution without the negative stain was mixed with a drop of the negative stain solution and then transferred to the carbon film and onto the grid and drained; (c) a drop of the lipid dispersion prepared in the NaCl solution without the negative stain was transferred to the carbon film and onto the grid, the excess solution drained with filter paper, and a drop of the negative staining solution was layered onto the grid and drained. The morphology of the different dispersions was very similar employing any of the three different procedures. However, a better contrast due to more complete penetration of the negative stain within the interlamellar spaces, uniformity of background and resolution was generally obtained when the lipid dispersions were prepared in 2% sodium phosphotungstate-NaCl (300

mosM final) according to procedure (a) and this was selected for routine observation with a Phillips EM 300 electron microscope operating with an objective aperture of 20 μm and accelerating voltage of 60 kV.

Measurement of the sizes of micelles, liposomes and of the hydrocarbon or aqueous interlamellar layers (i.e., the dark and clear layers representing, respectively, the zones penetrated by the aqueous solution containing the negative stain and those not) was done on suitably enlarged photographs of the dispersions using a magnifying ocular lupe (10 ×) having a graduated scale. For determining average sizes of the structures, population distribution and lamellar thickness or spacings, 200 measurements were done for each sample in different fields of at least two different preparations and the values were averaged. The standard deviations of these values were within a maximum of ±15% of the averages given for any of the preparations. Theoretical calculations of the predicted thermodynamic and geometric parameters for single or two-component systems were done with a computer program running an iterative algorithm to convergence according to the theory of self-assembly of hydrocarbon amphiphiles [3] previously adapted to these systems [5].

Results

Single-component systems

(a) Neutral glycosphingolipids. Fig. 1 shows the morphology and size distribution of liposomes formed by neutral glycosphingolipids. The multilamellar vesicles show a clear tendency to become smaller and more homogeneous in size as the oligosaccharide chain of the glycosphingolipids is longer.

GlcCer forms large vesicles; 83% of these have a diameter above 100 nm and 25% of the total are above 500 nm. The morphology for the GalCer vesicles is similar. Occasionally, flattened multilamellar structures or tubules with a diameter of about 50–100 nm can be observed. These structures for systems containing cerebrosides were described before [18–20]. Under the same conditions, multilamellar vesicles of DPPC (not shown) reveal sizes in which 96% of the structures are above 100 nm diameter with 44% of the total with a diameter between 500 and 700 nm. In the case of LacCer, 87% of the vesicles have a diameter below 300 nm and the distribution is more homogeneous since only 19% of them have a diameter below 80 nm while 73% have diameters in the 80–300 nm range. The vesicles are smaller and the distribution even more homogeneous for Gg_3Cer and Gg_4Cer for which 97% and 99% of the vesicles correspond to sizes between 40 and 100 nm and 20 and 80 nm, respectively. Both the spacings corresponding to the hydrophobic layer and the aqueous interlamellar period increase as the oligosaccharide chain is longer. The values for GlcCer, LacCer, Gg_3Cer and Gg_4Cer are 4.3, 4.7, 4.8, and 5.1 nm for the hydrocarbon layer and 1.5, 2.0, 2.5, and 2.8 nm for the aqueous space, respectively.

Fig. 2a compares the radius of curvature of vesicles formed by the different neutral glycosphingolipids; the values correspond to the maxima of the distribution histograms in the corresponding photographs of Fig. 1. The radius of curvature theoretically expected for the same glycosphingolipids on the basis of their molecular geometry [5] are also shown in Fig. 2a at two different lateral surface pressures. As can be seen, variations of the values of surface pressure at which the theoretical radii are calculated do not modify the general agreement with the experimental data nor the dependence of the radius of curvature with the type of glycosphingolipids. It should, however, be pointed out that the surface pressure may show important fluctuations about the average value [23], especially for the more liquid expanded glycosphingolipids [22]. The average values of surface pressure more relevant to biomembranes are probably about 30 $mN \cdot m^{-1}$ or above [4,21].

(b) Anionic glycosphingolipids. Fig. 1 also shows the morphology of negatively stained dispersions of sulfatide and gangliosides of different complexity. Sulfatide reveals multilamellar vesicles of a size similar to those of GlcCer, GalCer or LacCer but usually containing fewer lamellae and with a greater spread of the size distribution. The thickness of the hydrocarbon layer is 4.8 nm and the aqueous interlamellar spacing is 2.0 nm.

The morphology of the ganglioside dispersions is very different since these lipids do not form vesicular structures. Gangliosides G_{M3} and G_{M2},

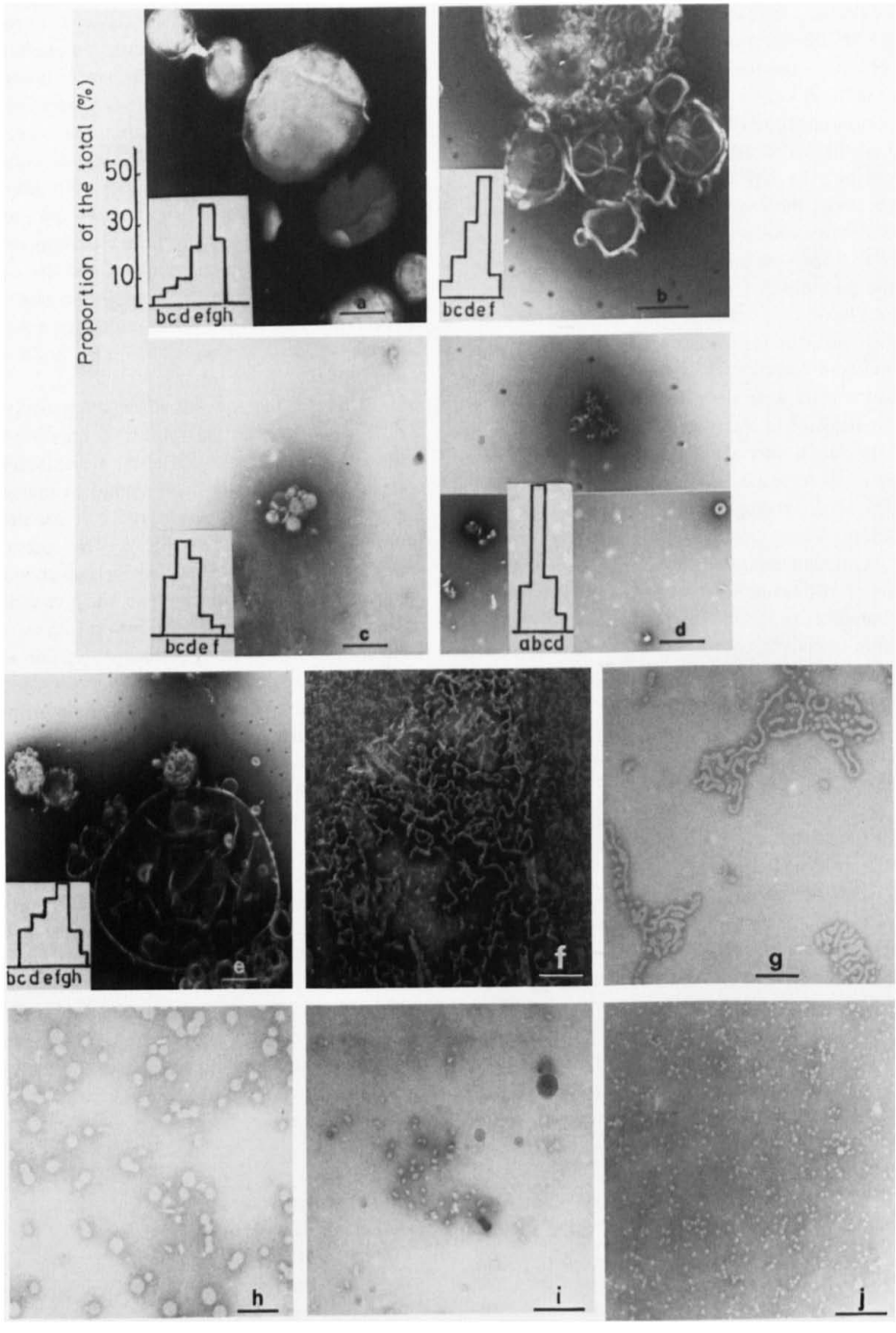
Proportion of the total (%)
50
30
10
bcdefgh
a
bcdef
b
bcdef
c
abcd
d
bcdefgh
e
f
g
h
i
j

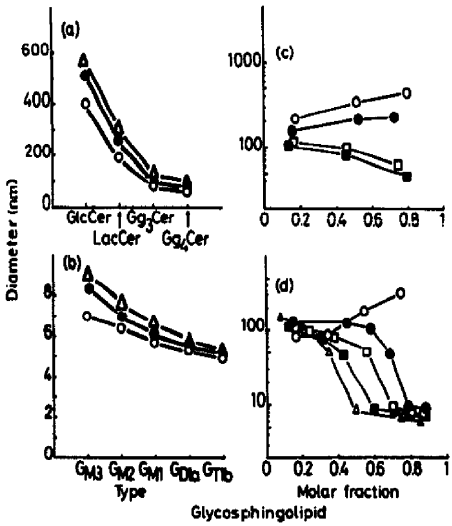

Fig. 2. Diameter of vesicles formed by individual glycosphingolipids and their mixtures with DPPC. Left: the diameters measured experimentally (●) or theoretically calculated at 30 $mN \cdot m^{-1}$ (○) and 35 $mN \cdot m^{-1}$ (△) are shown for the individual neutral glycosphingolipids (a) and gangliosides (b). Right: the diameters experimentally measured in preparations containing DPPC and neutral (c) or anionic (d) glycosphingolipids at different molar fractions are shown for GalCer-DPPC (○); LacCer-DPPC (●); Gg_3Cer-DPPC (□); Gg_4Cer-DPPC (■); sulfatide-DPPC (○); G_{M3}-DPPC (●); GM_1-DPPC (□); G_{D1a}-DPPC (■) and G_{T1b}-DPPC (△).

with the shorter oligosaccharide chains of the series, form micelles of varied geometry. Three general structures can be visualized: small spherical micelles of an average diameter of 7.2 nm for G_{M3} and 6.8 nm for G_{M2}; globular or toroidal micelles of an axial ratio of about 2.4 for G_{M3} and about 2.9 for G_{M2} or long cylindrical micelles of wavy appearance. The shorter micelles have a tendency to stack together. The cylindrical micelles have an average diameter of 7.3 nm for G_{M3} and 6.9 nm for G_{M2}; the length is variable and ranges from about 38 nm to 120 nm, these micelles usually tend to stack although this is more frequently seen for G_{M3} than for G_{M2}. Long, wavy cylinders of more than 200 nm are also seen which often show lateral merging or fusion with similar structures. The photographs in Fig. 1 show a varied range of lengths for these micelles while the diameters are very similar for all the structures; this suggests that the different types of micelles arise either from rupture of the long cylindrical structures into smaller micelles or by fusion of the small spherical and globular micelles into the larger structures. When the cylinders are relatively short they are apparently stabilized by stacking. The aqueous spacings among the stacking micelles is about 2.4 nm.

For ganglioside G_{M1}, the predominant structures are the spherical and the globular or toroidal micelles. The average diameter of the smallest spherical micelles is 6.1 nm and the axial ratio of the corresponding globular micelles is 2.4 to 2.8. Spherical and globular micelles slightly bigger than these are also seen and probably correspond to structures formed by fusion or tight aggregation of between two and four smaller micelles. The micelles formed by G_{D1a} and G_{T1b} are even smaller than those of G_{M1} and become difficult to resolve. Mostly spherical or elipsoidal micelles with an average diameter of 5.6 nm for G_{D1a} (axial ratio about 1.9) and 4.9 nm for G_{T1b} are observed. Fig. 2b shows that the more frequent shapes observed are in reasonable agreement with theoretical expectations.

Fig. 3a shows that when the lateral surface pressure acting on the molecules is increased, the theoretical values for the radius of curvature of bilayer vesicles of neutral glycosphingolipids or ganglioside micelles become greater. This is because for a roughly similar hydrocarbon chain volume and length, the cross-sectional mean molecular area is less at higher lateral pressures [22] and the molecules become less wedge-shaped,

Fig. 1. Negative stain electron micrographs of aqueous dispersions of neutral and anionic glycosphingolipids. GlcCer (a); LacCer (b); Gg_3Cer (c); Gg_4Cer (d); sulfatide (e); G_{M3} (f); G_{M2} (g); G_{M1} (h); G_{D1a} (i) and G_{T1b} (j). The bars represent 200 nm in a, b, c, d and e; 100 nm in f; 80 nm in g, i and j; 40 nm in h. The histograms of the size distribution for the diameters measured by the scale shown in (a) are given for each of the preparations containing bilayer vesicles; the diameter distribution for micelles was homogeneous around the size given in the text. The letters in the abscissa of the histograms correspond to the following size ranges: 20–40 nm (a); 41–60 nm (b); 61–80 nm (c); 81–100 nm (d); 101–300 nm (e); 301–500 nm (f); 501–700 nm (g); 701–900 nm (h).

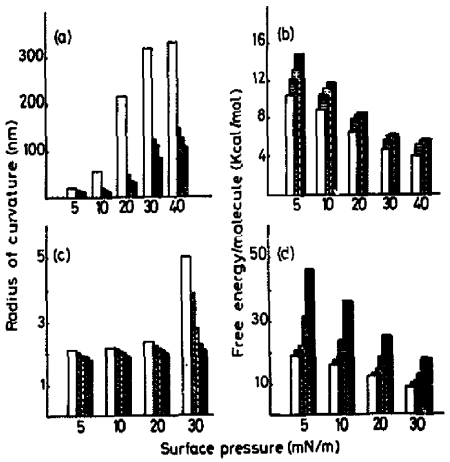

Fig. 3. Radius of curvature and free energy per molecule of structures of individual glycosphingolipids. The theoretically calculated radius of curvature (a and c) and free energy per molecule (b and d) at the surface pressure indicated are shown for bilayer vesicles of the following neutral glycosphingolipids (a and b): GlcCer (white bars); LacCer (lined bars); Gg_3Cer (dotted bars); Gg_4Cer (black bars); or for micelles (c and d) of the gangliosides G_{M3} (white bars); G_{M2} (stappled bars); GM_1 (dotted bars); G_{D1a} (lined bars); and G_{T1b} (black bars).

thus admitting a more favorable parallel intermolecular packing (see Ref. 5 and discussion below). At each pressure, the predicted radii are smaller for the glycosphingolipids with the longer oligosaccharide chain. Concomitantly, the theory indicates that the free energy of the molecule at the surface becomes greater for vesicles or micelles with the smaller radius (Figs. 3b, d).

Two-component systems

(a) Neutral glycosphingolipids. Neutral glycosphingolipids have the effect of lowering the average radius of multilamellar vesicles of DPPC according to their proportion (Fig. 4). In the presence of GlcCer (or GalCer) the diameter of the vesicles is shifted to below 500 nm compared to the more frequent sizes of vesicles of about 500–700 nm observed for DPPC alone (see the above section). This is in agreement with recent observations performed in mixed systems of purified cerebrosides and DPPC [18]. At a molar fraction of GlcCer of 0.177, about 62% of the total population of vesicles is below 500 nm. Increasing the proportion of GlcCer introduces little variation but there is a tendency to slightly increase the vesicle diameter as shown in Figs. 2c and 4. At molar fractions of GlcCer of 0.52 there are clearly two predominant populations of vesicles with 32% of them in the range of 60–100 nm and 40% between 100 and 500 nm. The vesicle population becomes again more homogeneous at a molar fraction of GlcCer of 0.80. A similar pattern was found for mixtures of DPPC with GalCer.

The variation of shape for mixtures of DPPC with LacCer is similar but the vesicular diameters are shifted to smaller values. The more frequent vesicles have sizes in the range of 100–300 nm depending on the amount of LacCer in the binary system (Figs. 2c and 4). Glycosphingolipids with three (Gg_3Cer) and four (Gg_4Cer) carbohydrate residues further reduce the size of the vesicles formed with DPPC. The more frequent vesicles for these mixtures are below 100 nm in diameter and this is further decreased by increasing the proportion of glycosphingolipids in the mixture; most vesicles containing Gg_3Cer or Gg_4Cer have diameters in the range of 20–80 nm at molar fractions of glycosphingolipids above 0.70 (Figs. 2c and 4). Some structures resembling flat stacked discs are seen for mixtures of DPPC and Gg_4Cer in these proportions.

(b) Anionic glycosphingolipids. The effect of sulfatide on the size of vesicles formed with DPPC is more marked than that of GlcCer or GalCer (Fig. 5). The diameter of most vesicles is about 100 nm for a molar fraction of sulfatide of 0.166. This size does not change much by increasing the

Fig. 4. Negative stain electron micrographs of aqueous dispersions of mixtures of neutral glycosphingolipids and DPPC at different molar fractions (X) of glycosphingolipids. GlcCer-DPPC: $X = 0.177$ (a); $X = 0.520$ (b); $X = 0.800$ (c). LacCer-DPPC: $X = 0.164$ (d); $X = 0.532$ (e); $X = 0.730$ (f). Gg_3Cer-DPPC: $X = 0.130$ (g); $X = 0.462$ (h); $X = 0.797$ (i). Gg_4Cer-DPPC: $X = 0.168$ (j); $X = 0.462$ (k); $X = 0.940$ (l). The bars represent 400 nm in c, e, i and j; 300 nm in l; 200 nm in a, b, d, f, g, h and k. The histograms of the size distribution for the diameters measured by the scale shown in (a) are given for each preparation. The letters in the abcissa of the histograms correspond to the sizes given in the legend of Fig. 1.

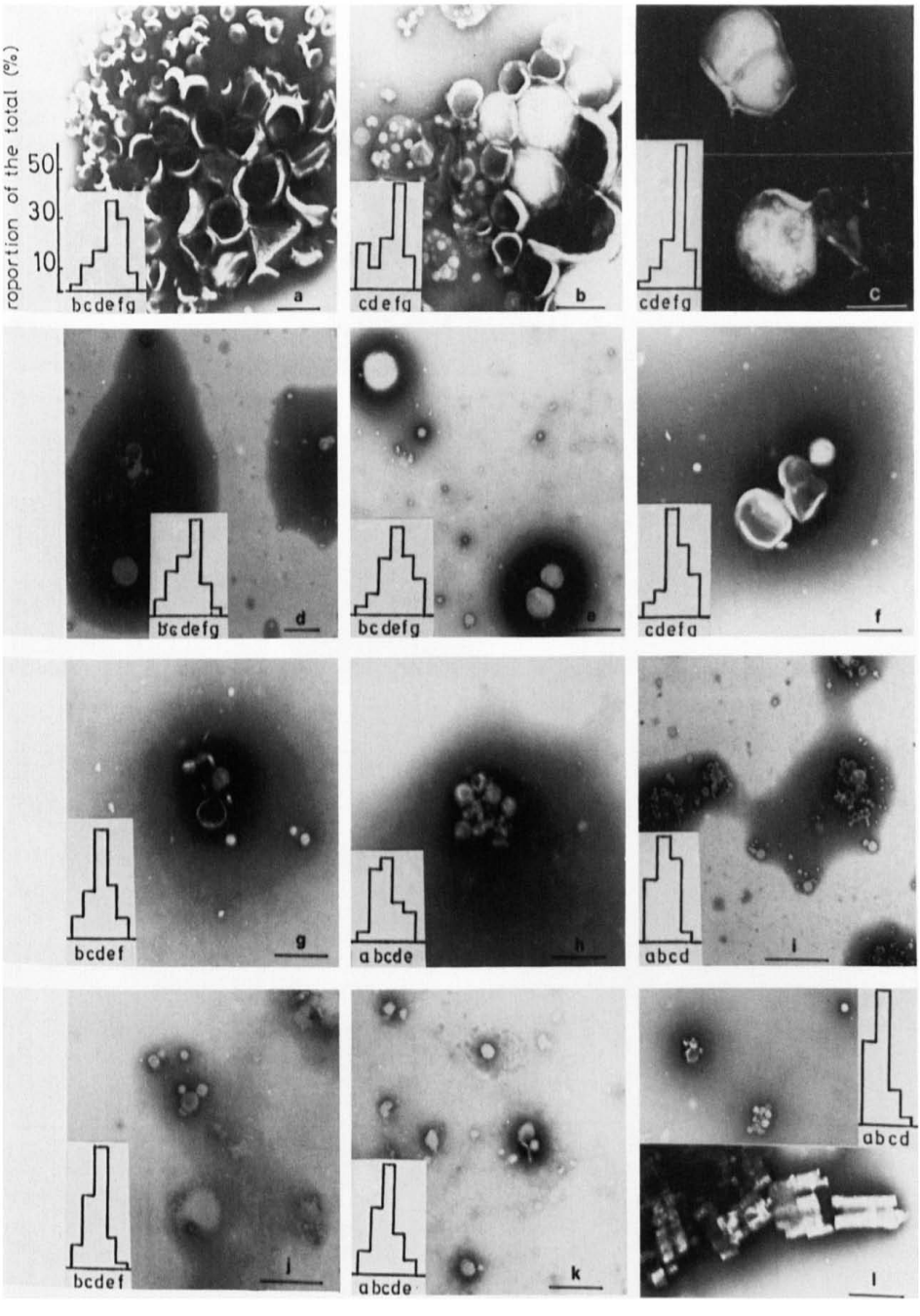
roportion of the total (%)
50
30
10
bcdefg
a
cdefg
b
cdefg
c
bcdefg
d
bcdefg
e
cdefg
f
bcdef
g
abcde
h
abcd
i
bcdef
j
abcde
k
abcd
l

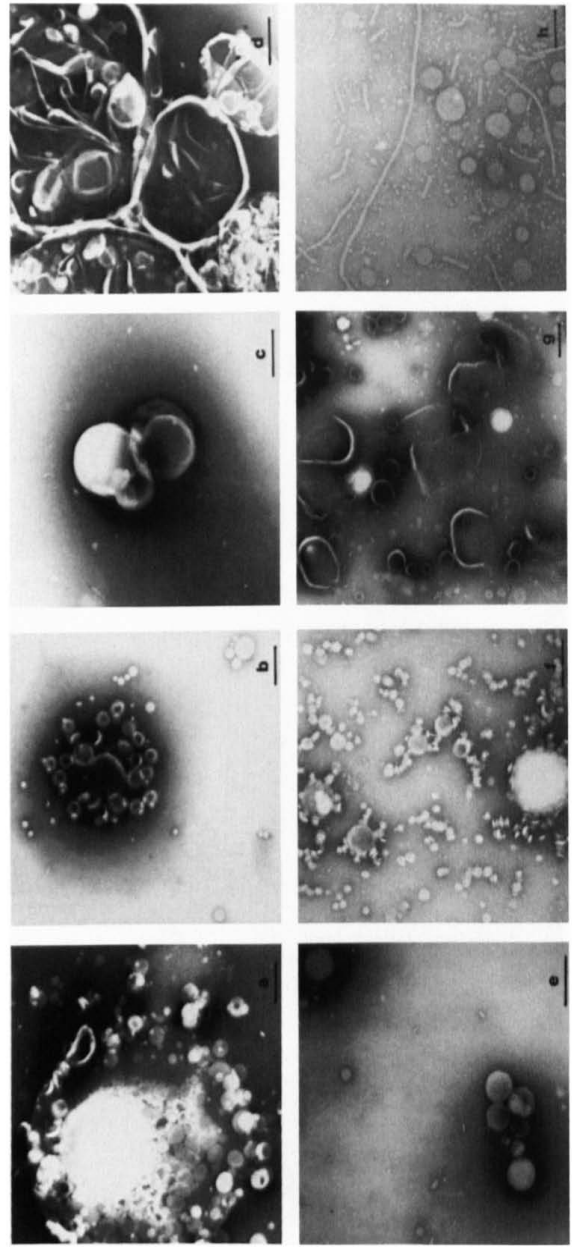
a
b
c
d
e
f
g
h

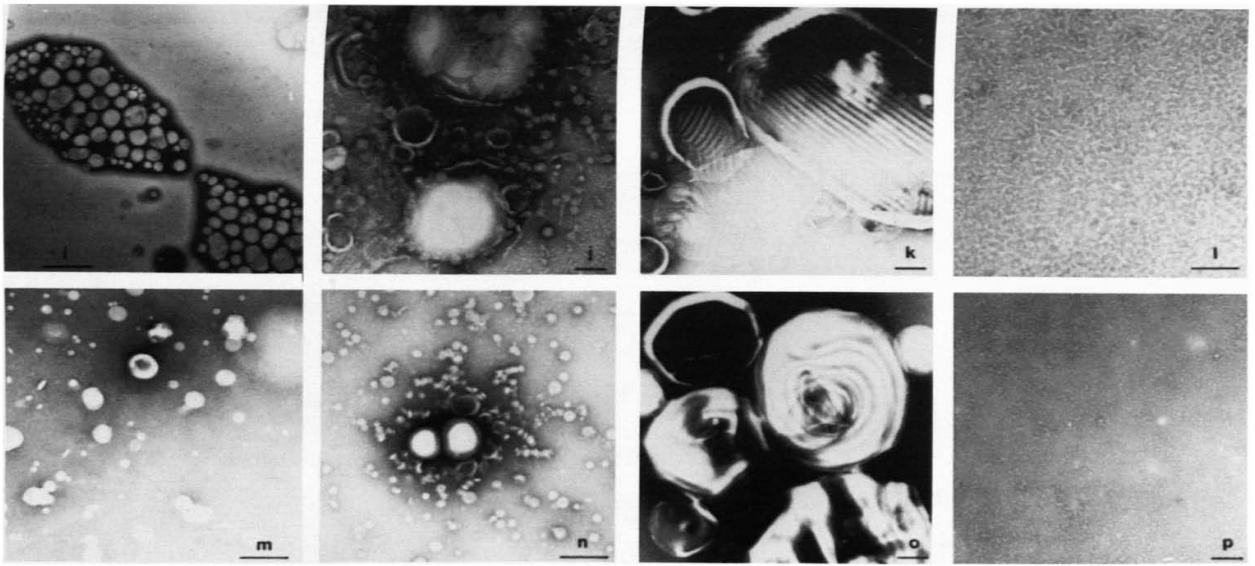

Fig. 5. Negative stain electron micrographs of aqueous dispersions of mixtures of anionic glycosphingolipids with DPPC at different molar fractions (X) of glycosphingolipids. Sulfatide-DPPC: $X = 0.166$ (a); $X = 0.344$ (b); $X = 0.545$ (c); $X = 0.750$ (d). G_{M3}-DPPC: $X = 0.150$ (e); $X = 0.580$ (f); $X = 0.580$ (g); $X = 0.787$ (h). GM_1-DPPC: $X = 0.170$ (i); $X = 0.380$ (j); $X = 0.380$ (k); $X = 0.710$ (l). G_{D1a}-DPPC: $X = 0.120$ (m); $X = 0.310$ (n); $X = 0.310$ (o); $X = 0.610$ (p). Preparations of G_{T1b}-DPPC were similar to those containing G_{D1a}. The bars represent 400 nm in f and g; 200 nm in a, b, c, d, e, i, k, l, m, n, o and p; 100 nm in h and j.

molar fraction of sulfatide up to about 0.50. Above this, an increase of the average size is induced (Figs. 2d and 5); most of the vesicles have diameters between 200 and 300 nm for a molar fraction of sulfatide of 0.545 and the size becomes bigger and more heterogeneous, with more frequent dimensions between 300 and 900 nm (Fig. 5) above a molar fraction of sulfatide of 0.70. As shown in Figs. 2d and 5, at molar fractions of G_{M3}, G_{M1}, G_{D1a} and G_{T1b} (not shown in Fig. 5) of 0.15, 0.17, 0.12 and 0.10, respectively, the size of the multilamellar vesicles is similar and most of the vesicles have diameters smaller than 200 nm. The distribution of sizes show a slight decrease in diameter as

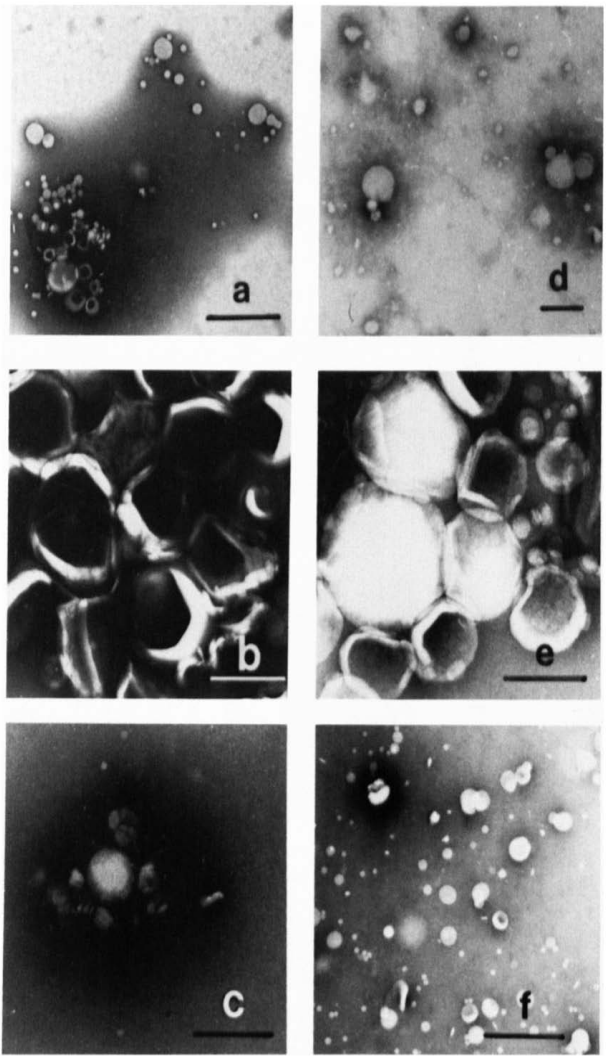

Fig. 6. Negative stain electron micrographs of aqueous dispersions of mixtures of GlcCer or Gg_4Cer with DPPC at different molar fractions (X) of glycosphingolipids. GlcCer-DPPC: $X = 0.570$ (a); $X = 0.650$ (b); $X = 0.740$ (c). GG_4Cer-DPPC: $X = 0.420$ (d); $X = 0.250$ (e); $X = 0.170$ (f). The bars represent 2000 nm in a; 1000 nm in b and f; 200 nm in c and e; 100 nm in d.

the molar fraction of gangliosides in the mixture is increased up to 0.35, 0.28, 0.18 and 0.14 for G_{M3}, G_{M1}, G_{D1a} and G_{T1b}, respectively. At these molar fractions remarkable morphological changes occur and two types of structures, vesicles and micelles, are observed (Fig. 5). As the amount of gangliosides is increased in the mixture the proportion of vesicles decreases while micelles become predominant. In addition, the size of the vesicles decreases (Fig. 2d) while the micelles show varied shapes such as cylindrical micelles of different lengths, globular micelles and small spherical micelles depending on the proportion of ganglioside (Figs. 2d and 5). Also, some structures resembling open vesicles or flattened sheets of considerable size (Fig. 5) are seen at molar fractions of 0.58 for G_{M3}, 0.38 for G_{M1}, 0.31 for G_{D1a} and 0.25 for G_{T1b} (not shown).

Fig. 6 shows that the vesicular diameter does not show a monotonical variation with composition but it exhibits maxima at certain proportions of glycosphingolipids. The more frequent vesicular diameter is in the range of 200–400 nm for DPPC-GlcCer ($X = 0.57$) and 50–100 nm for DPPC-Gg_4Cer ($X = 0.42$); it increases to the range of 500–700 nm for DPPC-GlcCer ($X = 0.65$) and to 100–300 nm for DPPC-Gg_4Cer ($X = 0.25$). The average vesicular radius then decreases to values

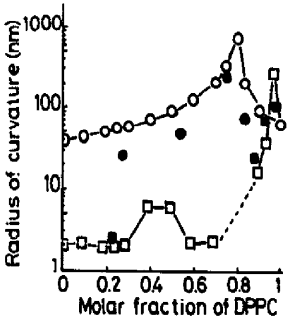

Fig. 7. Radius of curvature of mixtures of glycosphingolipids with DPPC. The theoretically calculated radius of curvature of bilayer vesicles formed by mixtures with DPPC at the molar ratios indicated are shown for Gg_4Cer-DPPC (○) or for G_{D1a}-DPPC (□). The dashed line in the latter system represents a region of composition where no structure can be predicted by the current theory (see Ref. 5). The experimentally measured values are shown with the corresponding black symbols.

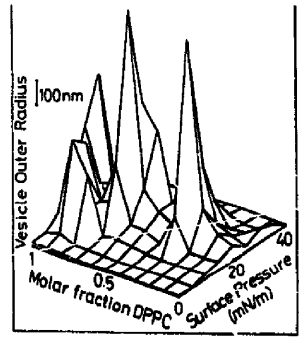

Fig. 8. Illustration of the variation of the radius of curvature with composition and surface pressure for GlcCer-DPPC.

in the range of 100–200 nm for DPPC-GlcCer ($X = 0.74$) and to 50–100 nm for DPPC-Gg_4Cer ($X = 0.17$). These results are comparable to the theoretical expectations shown in Fig. 7. In addition, the theory predicts that the radius of curvature will depend on the surface pressure and marked variations of the vesicular geometry may occur by small changes of composition and intermolecular packing (Fig. 8 illustrates this feature for the system GlcCer-DPPC, the general behavior of other systems is similar).

Discussion

The results described here clearly show that the type of oligosaccharide chain in neutral and anionic glycosphingolipids and their proportions in mixtures with DPPC have a remarkable influence on membrane morphology. These properties have profound effects in determining the final stability and the very existence of a bilayer membrane. This is consistent with previous theoretical analysis and several experimental studies [5–11, 18,49].

Single-component systems

Both theoretical and experimental observations (Figs. 1 and 2) show that neutral glycosphingolipids can form bilayer structures with a radius of curvature decrease in the order GlcCer = GalCer > LacCer > Gg_3Cer > Gg_4Cer. This is because the polar head group size, protrusion and optimal area

exposed to the aqueous phase in relation to the volume of the hydrocarbon portion determines a molecular shape further away from a cylinder and more similar to a cone as the glycosphingolipids are more complex [22,51].

For glycosphingolipids with short oligosaccharide chains such as GlcCer and GalCer the packing constraints allow the formation of rather large bilayer vesicles. This is determined by both the entropy of the system and the molecular geometry; the latter is measured by the critical packing parameter ($v/a_o l_c$) that relates the optimal cross-sectional molecular area a_o, the hydrocarbon chain volume v and the maximal hydrophobic length l_c [3]. These bilayers are stable since the free energy per molecule at the surface is low but the competing factor for a bigger size is entropy. This establishes an upper limit for the aggregation number compatible with the entropy of the aqueous phase that continuously favors maximal lipid aggregation in order to minimize the lipid/water interface. If the lateral surface pressure is decreased below 20 $mN \cdot m^{-1}$, the area per polar head group exposed to water increases in relation to the hydrocarbon chain volume. In this case, the critical packing parameter decreases [5] and the surface free energy per molecule acquires higher values (Fig. 3). Even if within certain limits this may not conflict with entropy, the molecular geometry becomes inadequate for the formation of large bilayer vesicles and these will spontaneously break into smaller ones. In a membrane, this can occur because the lateral surface pressure is a fluctuating parameter that introduces periodical tangential stress and variations of compressibility [23] along the membrane plane. This affects and is, in turn, modified by other factors that can control morphology such as the phase state and intermolecular interactions in the hydrocarbon and polar head group region [17,24,26]. Effects of this type may explain the observed heterogeneous population of vesicles and morphological changes induced by temperature variations [27].

For LacCer, Gg_3Cer and Gg_4Cer the critical packing parameter still allows the formation of bilayer vesicles but both the molecular geometry and entropy are more compatible with a smaller size; these are the structures observed (Figs. 1 and 2) even if the system must then concede a higher free energy per molecule (Fig. 3). Similar factors operate when the oligosaccharide chain exceeds a certain size or suffers changes in orientation with respect to the hydrocarbon portion. In practice, this has the same effect as altering the hydrophilic-hydrophobic length balance for optimal stability [22] or the molecular area exposed to water. A different conformation of the polar head group also had a marked influence on the morphology of the structure. The conformation of globoside (Gb_4Cer) with an L-bent oligosaccharide chain compared to the straight conformation of asialo-G_{M1} (Gg_4Cer) leads to a larger value of the cross-sectional molecular area in relation to the hydrocarbon portion [28]. This determines a critical packing parameter no longer compatible with the formation of bilayer vesicles. Thus, globoside forms cylindrical micelles in aqueous dispersions [29] while Gg_4Cer can still form vesicles. Sulfatide forms vesicles similar to GlcCer, GalCer and LacCer with radii that are within the ranges predicted by theory but rather more disperse in size (Fig. 1).

For gangliosides, the molecular geometry determines critical packing parameters that are well out those allowing the formation of bilayer vesicles and only micelles of different shapes are found (Figs. 1 and 2). Values for the critical packing parameter for all these systems at different surface pressures were previously published [5]. The geometrical features and aggregation number of micelles formed by gangliosides G_{M3}, G_{M2}, G_{M1}, G_{D1a} and G_{T1b} were previously calculated with the Israelachvili model [5] employing the experimentally determined molecular parameters [22]. Recently, these features were experimentally measured in a series of studies using laser light scattering and small angle neutron scattering [8,30,31]. With these studies, precise data on the molecular weight, hydrodynamic radius and axial asymmetry were obtained for the above ganglioside series. These results are in agreement with the theoretical predictions reported [5] and with the observations made in the present work (Figs. 1 and 2).

Compared to the other gangliosides, G_{M3} and G_{M2} contain the shorter oligosaccharide chains and have the smaller cross-sectional areas in relation to the hydrocarbon portion [22]; their critical packing parameter is similar and out of the range

in which bilayer vesicles are permitted but it is compatible with the formation of cylindrical micelles [5]. These structures of variable length are abundantly observed (Fig. 1). However, smaller eliptical or toroidal and spherical micelles are also seen. Obviously, entropy constraints set an upper limit for the aggregation number; cylindrical micelles formed either spontaneously or by subsequent fusion of smaller structures (see Results) have lengths that are rarely beyond 700 nm. The structures formed by these gangliosides are similar to those described for globoside [29].

As the ganglioside oligosaccharide chain becomes more complex (e.g., G_{M1}, G_{D1a} and G_{T1b}) the critical packing parameter takes progressively smaller values [5]. Elipsoidal and globular or toroidal shapes are frequently seen for G_{M1} and G_{D1a} and small spherical micelles for G_{T1b} (Fig. 1). The axial ratio and the aggregation number for the elipsoidal shapes are in good agreement with the values predicted by theory (Fig. 2, Ref. 5) and with the axial ratios and molecular weights determined by radiation scattering [8,31]. As expected, the surface free energy per molecule is higher for the smaller structures and, even more, at lower lateral surface pressures (Fig. 3); this is because the cross-sectional area exposed at the hydrocarbon/water interface becomes greater for the gangliosides with longer oligosaccharide chains and at lower lateral pressures [22]. However, except for gangliosides G_{M3} and G_{M2} above 20 $mN \cdot m^{-1}$, this has little influence on the possibilities for variation of the radius of curvature of the corresponding micelle (Fig. 3). This is because for the more complex gangliosides both the molecular geometry and the entropy factor favor a highly curved shape with almost no flexibility for packing variations. Actually, these structures are in the very limit of their thermodynamic and geometrical possibilities for maintaining an aggregated state. More imbalance in the hydrophilic character or size of the polar head group in relation to the hydrocarbon portion, a relatively large fluctuation of the lateral pressure (or variations of the polar head group orientation) result in vanishingly small intermolecular interactions and these molecules become soluble [17,36]. This may also explain the considerable tendency of ganglioside micelles to exhibit a rather fast transfer of monomeric gangliosides to bilayer vesicles described recently [32,33].

Two-component systems

When two different classes of lipid form the aggregate the competing thermodynamic and geometric constraints may, in principle, be more easily satisfied by an asymmetrical localization of the two different molecules in the two halves of a bilayer membrane. Apart from the individual molecular geometry, two intimately related constraints, one acting at short-range and the other at long-range have to be further balanced in this case. The first refers to the establishment of (favorable or unfavorable) intermolecular interactions that may result, in addition, in miscibility or immiscibility of surface domains at a longer range [24,26,34]. If immiscibility occurs, then individual shape constraints acting on the different compositional domains also have to be thermodynamically and geometrically compatible. The second consists of the progressive build-up of an unfavorable entropy term arising from the demixing process between the inner and outer monolayer of the bilayer membrane as the asymmetry in composition increases to satisfy the different molecular geometries.

The critical packing parameter of GlcCer, GalCer, LacCer and sulfatide allows for the formation of stable bilayer vesicles whose more frequent sizes are smaller but still in the range of those found for DPPC and, therefore, vary little with composition. In systems of DPPC-GalCer, it has been found that the type of fatty acyl chain in the ceramide moiety further influences the membrane morphology [18]. For mixtures of DPPC with Gg_3Cer and Gg_4Cer the more different molecular geometry induces changes of the vesicular radius of curvature, especially at higher proportion of the glycosphingolipids (Figs. 2 and 4). These shapes are in agreement with the variations predicted by theory (see also Fig. 7).

For systems containing gangliosides, the geometrical stress introduced by the markedly different molecular parameters of gangliosides and DPPC cannot be relieved by asymmetry beyond a certain composition. In general, bilayer vesicles are possible only for a limited amount of gangliosides. These structures are always much smaller

than the vesicles formed by DPPC alone or mixed with neutral glycosphingolipids and tend to slightly reduce their size as the proportion of gangliosides increases and as the oligosaccharide chain in the ganglioside becomes more complex (Figs. 2 and 5). More than 80% of the gangliosides have been previously found to be accessible to chemical reagents on the external surface of bilayer vesicles formed by mixtures of ganglioside with DPPC [11,35,37]. When the proportion of ganglioside reaches a certain value a drastic structural rearrangement takes place and cylindrical, elipsoidal and spherical micelles are formed. These micelles coexist with bilayer vesicles over a certain range of composition but as the proportion of gangliosides increases the amount of vesicles decreases rapidly and, beyond a certain point, only micelles remain. The different shapes and ranges of coexistence are in good agreement with studies by radiation scatter and high sensitivity differential calorimetry performed with some of these systems [25,26,30,49] and are adequately predicted by the Israelachvili model [5].

An interesting phenomenon is that the radius of curvature of the vesicular structures formed by glycosphingolipids and DPPC does not exhibit a monotonical variation (either always increasing, remaining invariant or always decreasing) with the composition but maximum values occur at particular molar fractions (see examples in Figs. 6 and 7). In the range of composition where this phenomenon is observed, the theoretical calculations employing the average molecular parameters of the individual lipids usually indicate that vesicular structures can not be formed because the critical packing parameter for the average molecule in the mixture exceeds 1.00 [5]. However, it has been shown that the interfacial stability, cross-sectional area, and orientation or length to which the oligosaccharide chain protrudes from the interface in relation to the hydrocarbon portion may vary considerably in a mixture of lipids. In addition, these parameters vary with the surface pressure, with the oligosaccharide chain conformation, with the type of interactions established with DPPC and other phospholipids and with the presence of water-soluble ligands [22,24,36–38].

As discussed elsewhere [5], these modifications can be taken into account in the theoretical model by three additional constraints: two geometric, related to the deviations of the values of mean molecular area and hydrocarbon volume in real systems compared to an ideal non-interacting mixture; and one thermodynamic, represented by the excess free energy of mixing compared to the ideal state [24]. If the cross-sectional molecular area in relation to the hydrocarbon chain length and volume used in the calculations is that experimentally measured for interacting systems [24], then the theoretical values also show the occurrence of peaks in the radius of curvature versus composition curve; these are in fair agreement with the experimental observations (Fig. 7) and will obviously depend on the lateral surface pressure at which the values for the molecular parameters are taken (Fig. 8). As theoretically expected, the hydrocarbon chains no longer remain in the same conformational state in these conditions and the phase state changes in these mixtures [25,26].

The theoretical calculations employing the molecular parameters of real interacting systems also predict that the structure will accept a greater proportion of gangliosides while still remaining in the form of a bilayer vesicle. The critical point of composition predicted by theory for a drastic structural rearrangement and formation of the micellar aggregate in mixtures with DPPC corresponds to molar proportions of about 35% for G_{M3}, 30% for G_{M1}, 20% G_{D1a} and 15% G_{T1b}. These values are very similar to those experimentally found for the region of coexistence of bilayer vesicles and micelles (Figs. 2d and 5) [25,26,30,36]. By contrast, if the molecular parameters employed to predict the morphology of the mixed system are those corresponding to an ideal mixture, the maximal proportion of gangliosides compatible with the formation of a bilayer vesicle are below 20% for G_{M3}, 15% for G_{M1}, 8% for G_{D1a} and 2% for G_{T1b} [5] and these values do not coincide with the experimental findings.

The reasonable agreement between theory and experimental data provides further evidence for the existence of a close correlation between the behavior of monolayers and bilayers in these systems [39] and for the general validity of the Israelachvili theory for describing the structural and thermodynamic behavior of simplified model membranes. The changes of membrane shape and

stability observed have biological implications and strengthen the concept that these lipids may be important for mediating, transducing or amplifying cell surface phenomena. The present results demonstrate directly the extreme sensitivity of the membrane morphology to what may be considered relatively small variations of the lipid composition, molecular structure or physical state. For example, the presence of a single additional carbohydrate residue in the oligosaccharide chain, a fluctuation of only 2 $mN \cdot m^{-1}$ in the surface pressure or a change in composition of less than 2 mol% can bring about dramatic changes of the radius of curvature and membrane stability. A 1% variation of the packing parameter for G_{M1} causes a 20% change in the molecular weight of the micelle [31]; the inclusion of an additional 2 mol% ganglioside in a mixed system with DPPC completely abolishes the pretransition endotherm of the phospholipid [26] and brings about changes of as much as 30–40% of the mean molecular area or surface potential per molecule [24]. This variation has remarkable and amplified consequences on the radius of curvature and structural stability.

On the other hand, the composition and physical state of the membrane will have to be adjusted if changes of the vesicular size or membrane curvature exceed the limits imposed to the system by the thermodynamic-geometric constraints. This may occur either by modifying the lateral and transverse topography [11] or by reorganizing into a different state of aggregation: this may either remain as a domain within the same general structure, adopt different local curvatures [5,34,35] or be forced to separate into the bulk phase. These phenomena may be important for explaining the composition-dependent shape variations of glycosphingolipid-containing membranes in the central nervous system during development [40,41]; also, they are probably involved in the formation of peculiar membranous bodies or lipid inclusions of particular morphology in hereditary sphingolipidosis when a certain amount of glycosphingolipid exceeds the stability limit for the membrane [42]; or in membrane vesiculation, fusion and instability brought about when the glycosphingolipid composition is altered in relation to other lipids in demyelinating diseases [36,43,44].

Furthermore, in a membrane with an heterogeneous glycosphingolipid composition each particular membrane region containing a defined population of molecules in certain proportions will probably tend to adopt its own constrained shape and features [5,34]. If these are mutually compatible within a general structure then localized variations of the radius of curvature may lead to transient protrusions and fluctuating membrane motions. If, on the other hand, the thermodynamic and geometric limits are exceeded then more drastic structural rearrangements in the form of tubules or membrane processes [18–20] vesiculation and fusion [45] or micellization will occur. In agreement with the above results, the glycosphingolipid composition and topography in different domains along the lateral or transverse membrane plane is different [11,46] although this is further regulated by the thermodynamic miscibility of each particular system [26,47]. Our results support the concept [48] that biological membranes containing these lipids should be represented as a mosaic of domains with different properties. These may rapidly adjust thermodynamically and morphologically to the actual intermolecular interactions within the membrane and with the external environment and have, in this manner, important functional consequences as multimolecular transducers or signal amplifiers.

Acknowledgments

R.K.Y. was supported by NIH grant NS-11843 and BM by grants from CONICET and CONICOR, Argentina.

References

1 Tanford, C. (1974) J. Phys. Chem. 78, 2469–2479.
2 Tanford, C. (1980) The Hydrophobic Effect, Wiley, New York.
3 Israelachvili, J.N., Mitchell, D.J. and Ninham, B.W. (1976) J. Chem. Soc. Farad. Trans. II 72, 1525–1568.
4 Israelachvili, J.N., Marcelja, S. and Horn, R.G. (1980) Q. Rev. Biophys. 13, 121–200.
5 Maggio, B. (1985) Biochim. Biophys. Acta 815, 245–258.
6 Barenholz, Y., Cestaro, B., Lichtemberg, D., Freire, E., Thompson, T.E. and Gatt, S. (1980) in: Structure and Function of Gangliosides (Svennerholm, L., Mandel, P., Dreyfus, H. and Urban, P.E., eds.), pp. 105–123, Plenum Press, New York.
7 Curatolo, W., Small, D.M. and Shipley, G.G. (1977) Biochim. Biophys. Acta 468, 11–20.
8 Corti, M., DeGiorgio, V., Ghidoni, R., Sonnino, S. and Tettamanti, G. (1980) Chem. Phys. Lipids 26, 225–238.

9 Bertoli, E., Masserini, M., Sonnino, S., Ghidoni, R., Cestaro, B. and Tettamanti, G. (1981) Biochim. Biophys. Acta 467, 196–202.

10 Felgner, P.L., Freire, E., Barenholz, Y. and Thompson, T.E. (1981) Biochemistry 20, 2168–2172.

11 Maggio, B., Montich, G.G. and Cumar, F.A. (1988) Chem. Phys. Lipids 46, 137–146.

12 Ando, S. and Yu, R.K. (1977) J. Biol. Chem. 252, 6247–6250.

13 Ledeen, R.W. and Yu, R.K. (1982) Methods Enzymol. 83, 139–191.

14 Ariga, T., Ando, S., Takahashi, A. and Miyatake, T. (1980) Biochim. Biophys. Acta 618, 480–485.

15 Kasai, N., Sillerud, L.O. and Yu, R.K. (1982) Lipids 17, 107–110.

16 Macala, L.J., Yu, R.K. and Ando, S. (1983) J. Lipid Res. 24, 1243–1250.

17 Maggio, B., Ariga, T., Sturtevant, J.M. and Yu, R.K. (1985) Biochemistry 24, 1084–1092.

18 Curatolo, W. and Neuringer, L.J. (1986) J. Biol. Chem. 261, 17177–17182.

19 McCarbe, P.J. and Green, C. (1977) Chem. Phys. Lipids 20, 319–330.

20 Lee, R.E., Worthington, C.R. and Glew, R.H. (1973) Arch. Biochem. Biophys. 159, 259–266.

21 Van Deenen, L.L.M., De Gier, J., Demel, R.A., De Kruijff, B., Blok, M.C., Van der Neut-Kok, E.C.M., Haest, C.W.M., Ververgaert, P.H.J.T. and Verkleij, A.J. (1975) Ann. N.Y. Acad. Sci. 264, 124–141.

22 Maggio, B., Cumar, F.A. and Caputto, R. (1978) Biochem. J. 175, 559–565.

23 Phillips, M.C., Graham, D.E. and Hauser, H. (1975) Nature 254, 154–155.

24 Maggio, B., Cumar, F.A. and Caputto, R. (1978) Biochem. J. 175, 1113–1118.

25 Sillerud, L.O., Schafer, D.E., Yu, R.K. and Konigsberg, W. (1979) J. Biol. Chem. 254, 10876–10880.

26 Maggio, B., Ariga, T., Sturtevant, J.M. and Yu, R.K. (1985) Biochim. Biophys. Acta 818, 1–12.

27 Hui, S.W., Stewart, T.P. and Yeagle, P.L. (1980) Biochim. Biophys. Acta 601, 271–281.

28 Maggio, B., Ariga, T. and Yu, R.K. (1985) Arch. Biochem. Biophys. 241, 14–21.

29 Pinteric, L., Tinker, D.O. and Wein, J. (1973) Biochim. Biophys. Acta 293, 630–638.

30 Masserini, M., Sonnino, S., Giuliani, A., Tettamanti, G., Corti, M., Minero, C. and DeGiorgio, V. (1985) Chem. Phys. Lipids 37, 83–97.

31 Cantu, L., Corti, M., Sonnino, S. and Tettamanti, G. (1986) Chem. Phys. Lipids 41, 315–328.

32 Brown, R.E., Sugar, I.P. and Thompson, T.E. (1985) Biochemistry 24, 4082–4091.

33 Brown, R.E. and Thompson, T.E. (1987) Biochemistry 26, 5454–5460.

34 Maggio, B., Fidelio, G.D., Cumar, F.A. and Yu, R.K. (1986) Chem. Phys. Lipids 42, 49–63.

35 Thomas, P.D. and Podder, S.K. (1982) Biochim. Biophys. Acta 688, 453–459.

36 Maggio, B., Cumar, F.A. and Caputto, R. (1981) Biochim. Biophys. Acta 650, 69–87.

37 Maggio, B., Monferran, C.G., Montich, G.G. and Bianco, I.D. (1987) in: New Trends in Ganglioside Research: Neurochemical and Developmental Aspects (Ledeen, R.W., Hogan, E.L., Tettamanti, G., Yates, A.J. and Yu, R.K., eds.), Fidia Research Series, Vol. 14, pp. 105–120. Liviana Press, Padova, Italy.

38 Bianco, I.D., Fidelio, G.D. and Maggio, B. (1988) Biochem. J. 251, 613–616.

39 Fidelio, G.D., Maggio, B. and Cumar, F.A. (1986) Biochim. Biophys. Acta 854, 231–239.

40 Wiegandt, H. (1985) in Glycosphingolipids (Wiegandt, H., ed.), pp. 199–260, Elsevier, Amsterdam.

41 De Robertis, F., Gershenfeld, H.M. and Wald, F. (1958) J. Biophys. Biochem. Cytol. 4, 651–667.

42 Andrews, J.M., Cancilla, R.A., Greppo, J. and Menkes, J.H. (1971) Neurology 21, 337–352.

43 Monferran, C.G., Maggio, B., Roth, G.A., Cumar, F.A. and Caputto, R. (1979) Biochim. Biophys. Acta 553, 417–423.

44 Roth, G.A., Roytta, M., Yu, R.K., Raine, C.S. and Bornstein, M.B. (1985) Brain Res. 339, 9–18.

45 Maggio, B., Cumar, F.A. and Caputto, R. (1978) FEBS Lett. 90, 149–152.

46 Tillack, T.W., Wong, M., Allietta, M. and Thompson, T.E. (1982) Biochim. Biophys. Acta 691, 261–270.

47 Thompson, T.E., Alietta, M., Brown, R.E., Johnson, M.L. and Tillack, T.W. (1985) Biochim. Biophys. Acta 817, 229–237.

48 Thompson, T.E. and Tillack, T.W. (1985) Annu. Rev. Biophys. Biophys. Chem. 14, 361–386.

49 Kojima, H., Hanada-Ypshikawa, K., Katagiri, A. and Tamai, Y. (1988) J. Biochem. 103, 126–131.